

Spin-Dependent Quasiparticle Transport in Aluminum Single Electron Transistors

A. J. Ferguson,* S. E. Andresen, R. Brenner, and R. G. Clark

*Australian Research Centre of Excellence for Quantum Computer Technology,
University of New South Wales, Sydney NSW 2052, Australia*

(Dated: September 2, 2018)

We investigate the effect of Zeeman-splitting on quasiparticle transport in normal-superconducting-normal (NSN) aluminum single electron transistors (SETs). In the above-gap transport the interplay of Coulomb blockade and Zeeman-splitting leads to spin-dependence of the sequential tunneling. This creates regimes where either one or both spin species can tunnel onto or off the island. At lower biases, spin-dependence of the single quasiparticle state is studied and operation of the device as a bipolar spin filter is suggested.

Quasiparticles often feature in the sequential tunneling processes of nanoscale superconducting devices. Examples include the Josephson quasiparticle resonances in superconducting single electron transistors (SETs) [1, 2], above-gap quasiparticle Coulomb blockade and even-odd parity effects on superconducting islands [3]. The quasiparticle has spin- $\frac{1}{2}$, however tunneling rates are not usually dependent on the orientation of this spin. One exception is in nanoscale aluminum islands with discrete energy levels where it is possible to directly study the quasiparticle spin state [5]. Spin dependent tunneling of quasiparticles has been important in large samples where efficient spin filtering may be performed [6, 7], and may be of interest for Coulomb blockaded samples where the behavior of single quasiparticle spins can be studied.

In this Letter we study the effect of Zeeman-splitting the quasiparticle states in lithographically fabricated normal-superconducting-normal (NSN) SETs. In order for Zeeman splitting to be observed in superconducting films, the effect of the magnetic field on the quasiparticle orbits must be suppressed. This is achieved by using ultra-thin (5 nm) aluminum films to confine the quasiparticle orbits, and precisely aligning the magnetic field in the plane of the film. This results in a spin-split quasiparticle density of states first observed by tunneling experiments in superconducting-normal tunnel junctions [6, 7]. In our samples the presence of a Zeeman energy (which can be comparable to both the charging and quasiparticle pairing energies), causes a difference in energy in creating spin-up and spin-down quasiparticle excitations on the device island and this leads to several spin-dependent transport regimes in the above-gap transport. In addition, quasiparticle populations with a well-defined spin are created on the island causing accumulation of a magnetic moment. In the below-gap transport, the Zeeman-splitting changes the energy of the spin- $\frac{1}{2}$ state of a single quasiparticle on the island. We observe this energy shift in the sequential tunneling processes and expect that operation of the device as a bipolar spin-filter will be possible.

The SETs were fabricated by electron beam lithography using a standard bilayer polymer resist and double angle evaporation process. The islands were made from

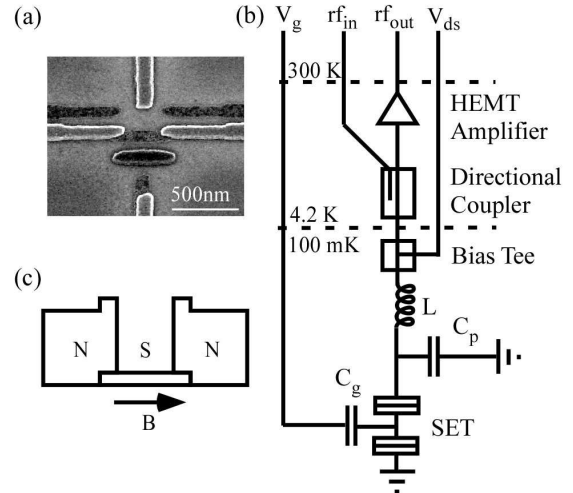


FIG. 1: (a) Micrograph of an SET similar to that measured, showing a difference in contrast between the 30 nm and 5 nm thick films. To avoid proximity effects, the normal-state leads do not contact their superconducting artifacts. (b) Simplified radio frequency circuit diagram. The $L = 470$ nH inductor and parasitic capacitance of $C_p = 0.42$ pF form a circuit with a resonant frequency of 321 MHz. (c) Schematic showing the relative thickness of the device leads and island. In a magnetic field of $B = 500$ mT, the leads are in the normal state while the island remains superconducting.

5 nm thick aluminum to allow Zeeman-splitting, while 30 nm thick aluminum was used for the leads. In order to achieve electrically continuous 5 nm films, the aluminum evaporation took place on a liquid nitrogen cooled stage with an evaporation rate of 0.15 nm s⁻¹. Between evaporation, the aluminum was oxidized at an oxygen pressure of 35 mTorr for 5 minutes to form tunnel barriers.

To enable rapid data acquisition and low noise measurement we configure the devices as rf-SETs [8]. The rf-SET technique involves impedance matching the relatively high SET resistance towards $50\ \Omega$ by embedding the devices in a resonant circuit (fig. 1(b)). At resonance, a reflective measurement of a small incident carrier signal ($V_{rf} \sim \mu$ V) is performed, with the reflected signal detected using a mixer circuit. This experimental set-

up is described in more detail in [9]. From the reflection coefficient and the tank circuit parameters, we can determine the SET differential conductance. High resistance SETs (181, 233 k Ω at 4.2 K) were chosen in order to reduce the effect of co-tunneling. As a consequence they were poorly impedance matched by our tank circuit. All measurements were performed in a dilution refrigerator which achieves an electron temperature of ~ 100 mK.

The in-plane critical magnetic field of aluminum is strongly dependent on film thickness [10]. By designing all-aluminum devices with 30 nm thick leads ($B_c < 0.5$ T) and a 5 nm thick island ($B_c = 3.8$ T), our superconducting SETs could be turned into normal-superconducting-normal (NSN) SETs by application of a magnetic field (fig. 1(a) & (c)). A limitation of this method is that we could only approximate a spin-degenerate NSN SET. We achieved this by applying a $B = 500$ mT in-plane magnetic field (fig. 2(a)). At this field, the Zeeman energy ($E_Z = g\mu_B B = 58$ μ eV) is greater than the thermal energy ($kT \sim 10$ μ eV) but the transport is not seriously modified from the spin-degenerate case since E_Z is still significantly less than the charging energy ($E_c = \frac{e^2}{2C_\Sigma} = 400$ μ eV) and the superconducting gap ($2\Delta = 680$ μ eV).

In NSN SETs the transport characteristics are determined by the energy required to create quasiparticle excitations, Δ , and the electrostatic charging energy. The main features are Coulomb diamonds, due to Coulomb blockade of quasiparticles on the island, which are offset from zero bias by $V_{ds} = \pm 2\Delta$ [11, 12]. Outside the blockaded regions, quasiparticle tunneling occurs, while in blockade, quasiparticle co-tunneling and low-rate sequential tunneling processes exist.

As the magnetic field is increased from $B = 500$ mT to $B = 2$ T, the Zeeman energy ($E_Z = 232$ μ eV) becomes comparable to E_c and Δ . Spin-up and spin-down (spin-down refers to spins antiparallel to the magnetic field and spin-up to spins parallel) quasiparticles now have significantly different energies on the device island. This makes the quasiparticle transport processes spin-dependent, causing the onset of quasiparticle tunneling to split (fig. 2(b)) and several new transport regimes (A-D) to emerge. The allowed transport processes for different bias conditions are determined by considering the spin-dependent free energy change for quasiparticles tunneling on and off the island [13].

We consider first quasiparticle transport for the device biased in region A. When the Coulomb blockade condition permits (determined by the total charge on the island at a particular time), a quasiparticle may tunnel from the drain onto spin-down above-gap states (fig. 3(a)). Above-gap states on the island filled in this way can also tunnel into the source causing a current to pass. In an analogous process for below-gap transport, spin-up filled states can tunnel into the source and quasiparticles from the drain can tunnel to fill the empty states. For

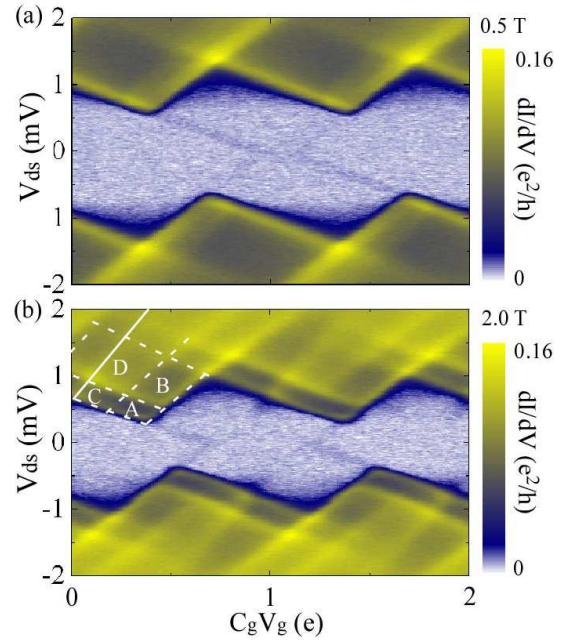


FIG. 2: Measurement of the Coulomb diamonds for the device in NSN operation as a function of magnetic field. V_g was ramped at 1 kHz and 256 averages were taken of each trace. (a) At $B = 500$ mT the device approximates an NSN SET. (b) Measurement taken at $B = 2$ T. The Zeeman-split density of states is seen in the above-gap transport as the emergence of new transport regimes at the onset of quasiparticle tunneling. The regions A-D between the white dotted lines correspond to transport regimes described in the text. The solid white line indicates an unknown spin-dependent transport process.

these bias conditions the resultant current has no net spin-polarization: a spin-down current flows above-gap and a spin-up current with the same magnitude passes through the below-gap states.

When biased in region A spin-down quasielectron and spin-up quasi-hole populations are generated on the island. Primarily this occurs since quasiparticle tunneling rates onto and off the island can be different with, for example, the tunneling rate from the above-gap filled states depending on the quasiparticle population [14]. A spin-up quasi-hole has the same magnetic moment as a spin-down quasielectron and this implies that a magnetic moment accumulates on the island as a result of the quasiparticle populations. In the following we estimate this bias dependent magnetic moment. Approximating to a flat superconducting density of states and for $V_{ds} - V_T(V_g) > kT$ (where $V_T(V_g)$ is the conduction threshold including both contributions from the superconducting gap and Coulomb blockade), the rate of above-gap quasiparticle tunneling onto the island through a tunnel barrier with conductance G is $\tau^{-1} \sim \frac{(V_{ds} - V_T)G}{2e}$. By contrast, the rate for each above-gap quasiparticle to tunnel off the island is given by

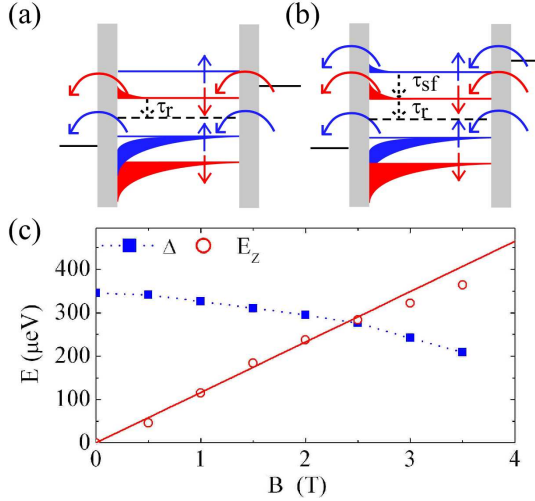


FIG. 3: (a)-(b) Quasiparticle tunneling processes that occur for the bias conditions A and B in fig. 2(b). Also shown schematically (dashed arrows) are possible recombination and spin-flip events. (c) The Zeeman-splitting ($E_Z = g\mu_B B$) and mean value of Δ as measured from above gap quasiparticle transport. A line fitted through the Zeeman splitting gives a g-factor of 2.01 ± 0.03 in the range $B = 0 - 2.5$ T (points at higher fields not included due to reduced fitting accuracy).

$\tau_{esc}^{-1} = \frac{G}{D_F e^2} \sim 100$ ns [14] where $D_F = 5.8 \times 10^6$ eV $^{-1}$ is the density of states at the Fermi energy for an island of dimensions 5 nm \times 100 nm \times 500 nm. Equilibrium is reached when the rates for quasiparticles tunneling on and off the island are equal, at which point the number of above-gap quasiparticles on the island is $N_{qe} = \frac{\tau_{esc}}{\tau}$. For $V_{ds} = V_T + 100$ μV (e.g. approximately in the middle of region A) and the average measured tunnel barrier conductance of $G = 11$ μS, $N_{qe} = 300$. An equal quasi-hole population leads to a magnetic moment $M = 600$ μB on the island. Quasiparticle recombination reduces these populations of quasielectrons and quasiholes, however, we expect that the recombination time is increased from the spin-degenerate case where $\tau_r = 1 - 10$ μs [15, 16] since a spin flip is required. Recombination was not considered in the estimate since $\tau_r > \tau_{esc}$.

We now discuss some of the features of regime B (fig. 3(b)), noting that C is similar except that the roles of the above and below-gap states are reversed. In B quasiparticles may tunnel into both the spin-up and spin-down above-gap states. However, there is an asymmetry with respect to the above- and below-gap states, and only spin-up quasiparticles may tunnel off the island from the below-gap states. There is an important difference in behavior between quasiparticles which tunnel into the spin-up and spin-down above-gap states. For the spin-up case there will be a fast spin-relaxation due to the availability of empty spin-down states at the same energy. This is similar to the case in normal state aluminium where the characteristic spin-flip time is $\tau_{sf} \sim 100$ ps [17]. By con-

trast, quasiparticles in the spin-down quasiparticles need to undergo an inelastic process for a spin-flip which we expect to have a much lower rate.

Finally, for regime D quasiparticles of both polarities are involved in both above and below-gap transport. However, the spin relaxation processes apply for the spin-up above and below-gap states as mentioned above. This relaxation will lead to a spin-imbalance on the device island. In this respect the quasiparticle transport behavior differs from that for a conventional SET with a spin-degenerate density of states.

By fitting the transport thresholds in Coulomb diamonds measured at magnetic fields from $B = 500$ mT to $B = 2.5$ T, we determined the quasiparticle g-factor to be $g = 2.01 \pm 0.03$. We also extracted Δ and found a modest reduction as a function of magnetic field due to residual orbital effects. The zero field value is $\Delta = 350$ μeV, which shows a strong enhancement over $\Delta \sim 200$ μeV for 30 nm films.

There are additional spin-dependent above-gap transport features, indicated by the solid line in fig. 2(b), that may involve co-tunneling processes. We do not analyze these features here but note that a master equation approach would be able to determine the processes involved [18]. All transport characteristics are reproduced in a second device of similar resistance and charging energy ($R = 233$ kΩ, $E_c = 475$ μeV).

We now consider the subgap transport processes near zero bias. If $E_c > \Delta$, as for our samples, an even-odd parity effect occurs as the system ground state alternates, as a function of gate voltage, between all Cooper-pairs and a state including a single quasiparticle [12]. In this parity effect the quasiparticle current is related to a thermal average number of quasiparticles on the island. Similar energy considerations also cause quasiparticle poisoning in single Cooper-pair transistors and Cooper-pair boxes. Close to $V_{ds} = 0$, the energy can be written as below. The term including $p(n)$ takes into account the energy required to create a quasiparticle excitation of either spin. If n , the number of quasiparticles on the island, is even, then $p(n) = 0$, while if n is odd, $p(n) = 1$.

$$E = \frac{(ne - C_g V_g)^2}{2C_\Sigma} + p(n)(\Delta \pm \frac{1}{2}g\mu_B B) \quad (1)$$

Figure 4(a) shows the Cooper pair and quasiparticle energy levels for $B = 2$ T as a function of gate bias. Since the spin-degeneracy of the quasiparticle states is lifted by the Zeeman energy, there are two parabolas representing the two quasiparticle spin states. Conductance maxima due to the sequential tunneling of quasiparticles occur at the degeneracies (fig. 4(b)). Their change in position with magnetic field reflects a spin-dependence caused by the Zeeman effect lowering the energy of the spin-down quasiparticle level. We note that this data, taken with 256 averages and time per trace of 500 μs, could have its

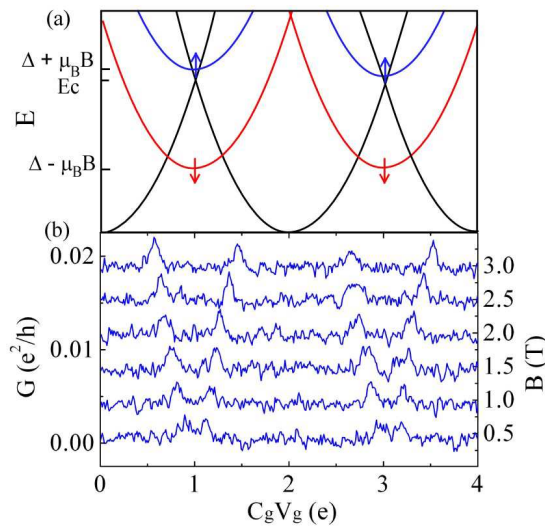


FIG. 4: (a) Energetics of Cooper pair and quasiparticle states at zero bias for $B = 2$ T. The experimental parameters $E_c = 475$ μ eV, $\Delta(B = 2T) = 295$ μ eV and $E_z = g\mu_B B = 238$ μ eV are used. The Cooper pair energy is unaffected by the magnetic field while the quasiparticle levels are split by the Zeeman energy. (b) Differential conductance (deduced from an averaged rf-measurement) at $V_{ds} = 0$ plotted as a function of B-field. The peaks move apart as the addition energy of a spin-down quasiparticle is lowered by the magnetic field.

signal-to-noise ratio significantly increased with further averaging and low-pass filtering.

We now examine the details of these transport processes, first considering the degeneracy between the 0-Cooper pair level and the spin-down 1-quasiparticle level. If the system is initially in the 0-Cooper pair state, a spin down quasiparticle may tunnel onto and then off, the island. This will result in a spin-down current. Sequential tunneling also occurs when the spin-down 1-quasiparticle state becomes degenerate with the 1-Cooper pair state. Now, a spin-up quasiparticle tunnels onto the island forming a singlet Cooper pair state with the spin-down quasiparticle already on the island. Subsequently a spin-up tunnels off, breaking a Cooper pair and leaving a single spin-down quasiparticle on the island. This gives rise to a spin-up polarized current. Between the degeneracies, a single above-gap spin-down quasiparticle remains on the island. The spin-polarization of these currents will be determined by the rate of spin-flip processes on the island and cotunneling events involving quasiparticles of the opposite polarity.

The ground state energetics indicate that the device can operate as a bipolar spin filter. This is analogous to similar behavior predicted in a GaAs quantum dot [19, 20], where the $n = 1$ electron Zeeman-split level filters spin-down electrons and the $n = 2$ singlet state filters spin-up electrons. There is a strong relationship between these cases since the Cooper pair is a spin singlet similar to the $n=2$ electron quantum dot ground state. For our

sample, the measured conductance is $G = 0.002 \frac{e^2}{h}$ and the peak width $V_{ds} \sim 100$ μ V, leading to a maximum current of ~ 10 pA. We suggest that it will be possible to obtain experimental confirmation of bipolar spin filtering by measuring the current through two independently tunable islands in series.

In conclusion, we have made use of the properties of thin-film aluminum to Zeeman-split the quasiparticle states on the NSN SET island. This leads to new spin transport regimes in both above- and below-gap transport. It will be interesting to further investigate the spin-filter effects in single and double island devices and perform studies of quasiparticle spin relaxation and recombination in these structures.

The authors thank D. J. Reilly, C. M. Marcus, B. J van Wees and F. E. Hudson for helpful discussions and D. Barber and R. P. Starrett for technical support. This work is supported by the Australian Research Council, the Australian government and by the US National Security Agency (NSA) and US Army Research Office (ARO) under contract number DAAD19-01-1-0653.

* Electronic address: andrew.ferguson@unsw.edu.au

- [1] T. A. Fulton et al., Phys. Rev. Lett. **63**, 1307 (1989).
- [2] Y. Nakamura, C. D. Chen, and J. S. Tsai, Phys. Rev. B **53**, 8234 (1996).
- [3] P. Lafarge et al., Phys. Rev. Lett. **70**, 994 (1993).
- [4] M. Tinkham, *Introduction to Superconductivity* (Dover, 2004).
- [5] D. C. Ralph, C. T. Black, and M. Tinkham, Phys. Rev. Lett. **78**, 4087 (1997).
- [6] R. Meservey, P. M. Tedrow, and P. Fulde, Phys. Rev. Lett. **25**, 1270 (1970).
- [7] P. M. Tedrow and R. Meservey, Phys. Rev. Lett. **27**, 919 (1971).
- [8] R. J. Schoelkopf et al., Science **280**, 1238 (1998).
- [9] T. M. Buehler et al., J. Appl. Phys. **96**, 4508 (2004).
- [10] R. Meservey and P. M. Tedrow, J. Appl. Phys. **42**, 51 (1971).
- [11] J. M. Hergenrother, M. T. Tuominen, and M. Tinkham, Phys. Rev. Lett. **72**, 1742 (1994).
- [12] T. M. Eiles, J. M. Martinis, and M. H. Devoret, Phys. Rev. Lett. **70**, 1862 (1993).
- [13] H. Grabert and M. H. Devoret, *Single Charge Tunneling*, (Plenum, New York, 1992) pp. 1-18.
- [14] F. W. J. Hekking et al., Phys. Rev. Lett. **70**, 4138 (1993).
- [15] J. L. Levine and S. Y. Hsieh, Phys. Rev. Lett. **20**, 994 (1968).
- [16] B. I. Miller and A. H. Dayem, Phys. Rev. Lett. **18**, 1000 (1967).
- [17] F. J. Jedema et al., Phys. Rev. B **67**, 085319 (2003).
- [18] G. Schön, J. Siewert, and A. D. Zaikin, Physica B **203**, 340 (1994).
- [19] P. Recher, E. V. Sukhorukov and D. Loss, Phys. Rev. Lett. **85**, 1962 (2000).
- [20] R. Hanson et al., Phys. Rev. B **70**, 241304(R) (2004).